Enhanced Ryanodine-Mediated Calcium Release in Mutant PS1-Expressing Alzheimer's Mouse Models

GRACE E. STUTZMANN,[a] IAN SMITH,[b] ANTONELLA CACCAMO,[b] SALVATORE ODDO,[b] IAN PARKER,[b] AND FRANK LAFERLA[b]

[a]*Department of Neuroscience, Rosalind Franklin University of Medicine and Science, The Chicago Medical School, Chicago, Illinois, USA*

[b]*Department of Neurobiology and Behavior, University of California, Irvine, California, USA*

ABSTRACT: Intracellular Ca^{2+} signaling involves Ca^{2+} liberation through both inositol triphosphate and ryanodine receptors (IP_3R and RyR). However, little is known of the functional interactions between these Ca^{2+} sources in either neuronal physiology, or during Ca^{2+} disruptions associated with Alzheimer's disease (AD). By the use of whole-cell recordings and 2-photon Ca^{2+} imaging in cortical slices we distinguished between IP_3R- and RyR-mediated Ca^{2+} components in nontransgenic (non-Tg) and AD mouse models and demonstrate powerful signaling interactions between these channels. Ca^{2+}-induced Ca^{2+} release (CICR) through RyR contributed modestly to Ca^{2+} signals evoked by photoreleased IP_3 in cortical neurons from non-Tg mice. In contrast, the exaggerated signals in 3×Tg-AD and $PS1_{KI}$ mice resulted primarily from enhanced CICR through RyR, rather than through IP_3R, and were associated with increased RyR expression levels. Moreover, membrane hyperpolarizations evoked by IP_3 in neurons from AD mouse models were even greater than expected simply from the exaggerated Ca^{2+} signals, pointing to an increased coupling efficiency between cytosolic [Ca^{2+}] and K^+ channel regulation. Our results highlight the critical roles of RyR-mediated Ca^{2+} signaling in both neuronal physiology and pathophysiology, and point to *presenilin*-linked disruptions in RyR signaling as an important genetic factor in AD.

KEYWORDS: IP3; endoplasmic reticulum; 2-photon; electrophysiology; calcium; Alzheimer; PS1; 3×Tg-AD; transgenic; ryanodine; cortex; neuron

Address for correspondence: Grace E. Stutzmann, Ph.D., Department of Neuroscience, Rosalind Franklin University of Medicine and Science, The Chicago Medical School, 3333 Green Bay Road, North Chicago, IL 60064. Voice: 847-578-8540; fax: 847- 578-8515.
grace.stutzmann@rosalindfranklin.edu

Ann. N.Y. Acad. Sci. 1097: 265–277 (2007).
doi: 10.1196/annals.1379.025

INTRODUCTION

Neuronal Ca^{2+} signaling is tightly controlled to ensure proper operation of a myriad of Ca^{2+}-dependent processes.[1,2] Two major sources contribute to cytosolic Ca^{2+} signals; an extracellular pool entering through plasma membrane channels, and an internal reservoir in the endoplasmic reticulum (ER) that is liberated by opening of inositol triphosphate- and ryanodine-receptor/channels (IP_3R and RyR). The activation of both IP_3R and RyR channels is promoted by cytosolic Ca^{2+}, resulting in a regenerative process of Ca^{2+}-induced Ca^{2+} release (CICR).[3–5] The feed-forward action of Ca^{2+} to enhance its own release through IP_3R and RyR introduces considerable complexity in Ca^{2+} signaling, and enables interactions between these different pathways.

Growing evidence implicates disruptions of Ca^{2+} signaling in the etiology of neurological diseases.[6–8] In particular, mutations in *presenilin* (*PS*) genes associated with Alzheimer's disease (AD) increase IP_3R-evoked Ca^{2+} release in a variety of cells.[9–11] Previous studies focused on responses evoked by elevating intracellular IP_3 either directly *via* flash photolysis of caged IP_3[10,11] or indirectly by agonist application,[9,12] and did not explicitly address the role of RyR in AD. Nevertheless, there is evidence pointing to RyR involvement. RyR expression levels are increased in cultured neurons expressing the $PS1_{M146V}$ mutation,[13,14] the RyR blocker dantrolene has been shown to reverse the elevated carbachol-induced Ca^{2+} release seen in SH-SY5Y cells expressing a mutant *PS1*,[15] and the RyR agonist caffeine evokes larger Ca^{2+} liberation in cultured neurons from transgenic AD mouse models.[14]

Here, we explore RyR involvement in neuronal functioning in both normal physiology, and during Ca^{2+} signaling disruptions associated with AD. For the latter purpose we employed two mouse models of AD: the $PS1_{M146V}$ mutant knockin, and a triple-transgenic mouse model ($3\times$Tg-AD).[16] Both transgenic mice display similarly exaggerated neuronal Ca^{2+} signals to IP_3 at all ages, but whereas the $PS1_{KI}$ mice fail to show AD histopathology, the $3\times$Tg-AD mice develop βA plaques and neurofibrillary tangles in an age- and a region-specific manner. We show that RyR activation contributes modestly to Ca^{2+} signals in nontransgenic (non-Tg) control mice, but accounts for almost all of the exaggerated ER Ca^{2+} signals in the $PS1_{KI}$ and $3\times$Tg-AD transgenic mice models. Moreover, in all groups, IP_3-dependent membrane hyperpolarizations are regulated primarily through RyR, and the transgenic mice show hyperpolarizing responses even greater than expected from the enhanced Ca^{2+} signals. Thus, RyR contribute largely to the exaggerated Ca^{2+} signals associated with AD-linked mutations in *presenilin*, and may thereby present a target for therapeutic intervention.

RESULTS

Exaggeration of IP_3-Evoked Ca^{2+} Signals in $PS1_{KI}$ and 3×Tg-AD Neurons

Individual neurons were loaded with caged IP_3 and fura-2 by dialysis through the patch pipette, and flashes of UV light of varying durations were applied to photorelease IP_3. The resulting ER Ca^{2+} liberation was monitored by imaging fura-2 fluorescence from the soma (excluding the nucleus) and the proximal dendrites using a custom-built 2-photon imaging system, and by measuring changes in membrane potential resulting from activation of Ca^{2+}-dependent K^+ channels. In addition, depolarizing current pulses were applied to evoke action potentials and accompanying entry of Ca^{2+} through VGCC.

FIGURE 1 A presents a scatter plot of individual IP_3-evoked responses evoked by selected flash durations, and FIGURE 1 B plots the mean amplitude of these responses as a function of flash duration (proportional to the amount of photoreleased IP_3) in the soma. The mean Ca^{2+} responses in $PS1_{KI}$ and 3×Tg-AD neurons were appreciably ($P < 0.05$) larger than in non-Tg control cells for all flash durations, with the greatest enhancement seen with 30 ms flashes (316% for $PS1_{KI}$ and 342% for 3×Tg-AD neurons); but were not significantly different from one another. In marked contrast, no significant differences in spike-evoked Ca^{2+} signals were apparent between non-Tg, $PS1_{KI,}$ and 3× Tg-AD groups ($P = 0.24$).

Enhanced RyR-Mediated Ca^{2+} Release Predominates in ER-Ca^{2+} Dysregulation

To ascertain the extent of the RyR-mediated component in the IP_3-evoked Ca^{2+} signals, we first determined the relative RyR contribution by comparing somatic signals evoked by photoreleased IP_3 (FIG. 2 A, B) before and after bath-applying 10 μM dantrolene to block RyR. In non-Tg neurons dantrolene caused a modest ($20 \pm 7\%$, $n = 6$) reduction in signals evoked by 50 ms flashes, and action potential-evoked Ca^{2+} signals were reduced by $15 \pm 5\%$. In marked contrast, dantrolene substantially reduced the IP_3-evoked Ca^{2+} responses in $PS1_{KI}$ neurons (by $59 \pm 11\%$, $n = 6$; $P < 0.01$) and in 3×Tg-AD neurons (by $71 \pm 9\%$, $n = 7$; $P < 0.01$). However, similar to non-Tg neurons, dantrolene produced only modest (15–20%) reductions of the spike-evoked Ca^{2+} signals.

The effects of dantrolene on the dose-response relationship for IP_3-evoked Ca^{2+} signals are shown in Figure 2 C. Responses in $PS1_{KI}$ and 3×Tg-AD neurons were not significantly different from one another ($P > 0.05$), and we therefore combined these data (Tg) for analysis. Dantrolene strongly suppressed Ca^{2+} signals in the pooled Tg neurons ($n = 19$) across the full range

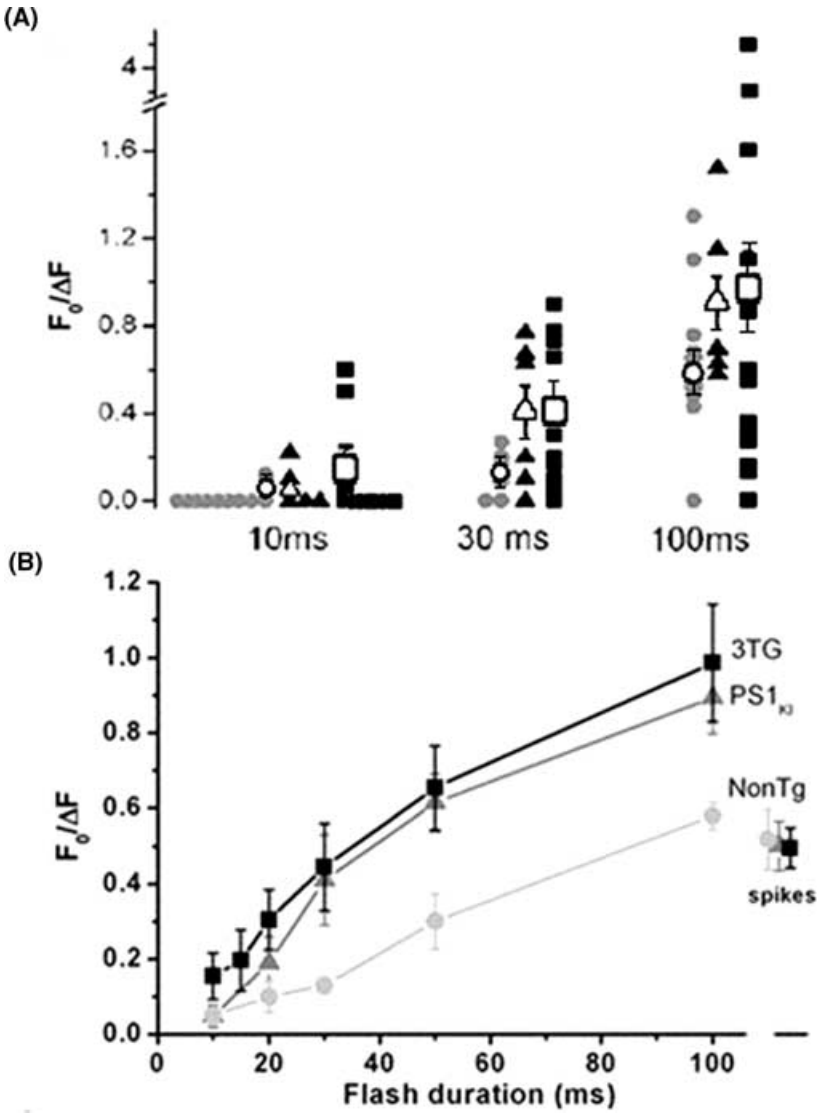

FIGURE 1. IP_3-evoked Ca^{2+} signals are exaggerated in both $PS1_{KI}$ and 3×Tg-AD mice. (**A**) Peak amplitudes of IP_3-evoked somatic Ca^{2+} signals evoked by photolysis flash durations of 10, 30, and 100 ms in individual non-Tg (*circles*), $PS1_{KI}$ (*triangles*), and 3×Tg-AD neurons (*squares*). Open symbols with error bars indicate corresponding means and standard errors. Average $PS1_{KI}$ and 3×Tg-AD Ca^{2+} amplitudes were significantly ($P < 0.05$) larger for the 30 and 100 ms flash durations relative to the non-Tg values. (**B**) Mean peak amplitudes of somatic Ca^{2+} signals as a function of photolysis flash duration; data are from 12–14 neurons for each group. Points at the right indicate mean Ca^{2+} signals evoked by action potential trains. Data from non-Tg mice are indicated by *light-gray circles* (●), $PS1_{KI}$ mice by *dark-gray triangles* (▲), and 3×Tg-AD mice by *black squares* (■).

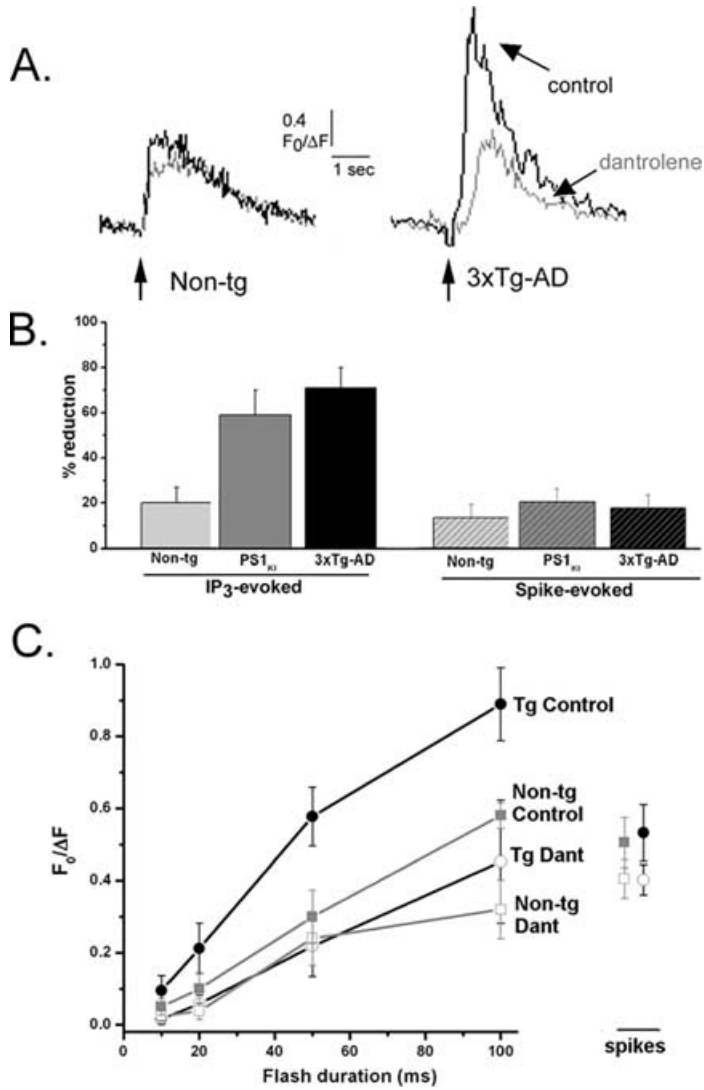

FIGURE 2. Ca^{2+} liberation through RyR contributes to the IP_3-evoked Ca^{2+} signals. (**A**) IP_3-evoked Ca^{2+} signals are reduced by the RyR blocker dantrolene. Traces show Ca^{2+} responses evoked by a 50 ms flash in control conditions (*black*) and in the presence of bath-applied dantrolene (*gray*), in representative non-Tg (*left*) and 3×Tg-AD (*right*) neurons. (**B**) Mean percentage reductions in amplitudes of IP_3-evoked Ca^{2+} responses (50 ms flash duration) and spike-evoked Ca^{2+} signals resulting from application of dantrolene (10 μM) in non-Tg ($n = 6$), $PS1_{KI}$ ($n = 6$), and 3×Tg-AD ($n = 7$) neurons. (**C**) Effect of dantrolene on the dose-response relationship of IP_3-evoked Ca^{2+} signals. Points show measurements from non-Tg neurons ($n = 12$; *squares*) and pooled measurements from 3×Tg-AD and $PS1_{KI}$ neurons (Tg, $n = 25$, *circles*) before (*filled symbols*) and after (*open symbols*) applying dantrolene. Data at the right show respective spike-evoked Ca^{2+} signals.

of flash durations tested (FIG. 2 C; circles), whereas the reduction in non-Tg neurons ($n = 6$) was less pronounced (FIG. 2 C; squares). Importantly, there were no significant differences ($P > 0.05$) between Tg and non-Tg groups in the Ca^{2+} signals remaining in the presence of dantrolene, suggesting that Ca^{2+} flux through the IP_3R channels themselves is not appreciably enhanced by the AD-linked mutations, but rather that larger responses in the Tg neurons arises principally from greater CICR through RyR. In contrast to the IP_3-evoked Ca^{2+} signals, spike-evoked Ca^{2+} signals were reduced to a similar extent in both the non-Tg and Tg neurons.

RyR Expression Levels Are Increased in Both $PS1_{KI}$ and 3 × Tg-AD Mice

We performed Western blot analyses of several Ca^{2+} signaling-related proteins in the brains of non-Tg, $PS1_{KI,}$ and 3×Tg-AD mice at ages (4–6 weeks) equivalent to those used in the imaging studies. There were no significant differences ($P = 0.46$) in cortical expression levels of IP_3R, SERCA-2B, calsenilin, calbindin-D, or calreticulin (data not shown). However, RyR levels were significantly enhanced (FIG. 3; ∼2-fold; ANOVA $F_{(2,8)} = 9.41$, $P \leq 0.01$) in the $PS1_{KI}$ and 3×Tg-AD mice relative to non-Tg controls (Fischer *post hoc* analysis, $P = 0.04$ and 0.005, respectively). RyR levels in $PS1_{KI}$ and 3×Tg-AD mice were not different from each other ($P = 0.14$).

IP_3-Evoked Membrane Hyperpolarization Is Driven by Ca^{2+} Liberation through RyR

IP_3 evokes a membrane hyperpolarization in cortical neurons *via* activation of Ca^{2+}-dependent K^+ channels[17,18] and this hyperpolarization is enhanced in

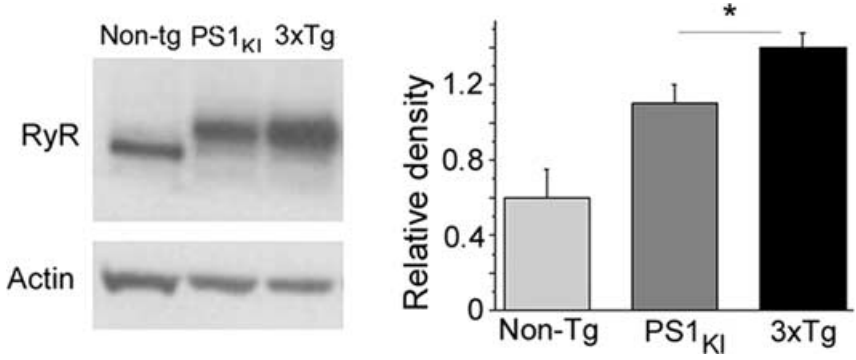

FIGURE 3. Tg neurons show enhanced expression of RyR and expression of mutant transgenes. *Left*: representative Western blots from homogenized non-Tg, $PS1_{KI,}$ and 3×Tg-AD cortices demonstrating differences in RyR levels relative to β-actin. *Right*: RyR levels in the $PS1_{KI}$ and 3×Tg-AD mice were significantly greater (∼2-fold) than non-Tg levels ($P < 0.05$), but were not different from each other.

$PS1_{KI}$ mice.[18,19] Here, we sought to determine whether the K^+ channel regulation primarily involves Ca^{2+} liberated through the IP_3R channels themselves, or is consequent to CICR through RyR channels.

Representative membrane potential responses to photorelease of IP_3 in non-Tg and 3×Tg-AD neurons are shown in FIGURE 4 A, and were appreciably smaller and of lower sensitivity in the non-Tg cells. These differences did not arise through differences in initial resting membrane potential (set to −60 mV by current injection) or input resistance. Strikingly, all responses

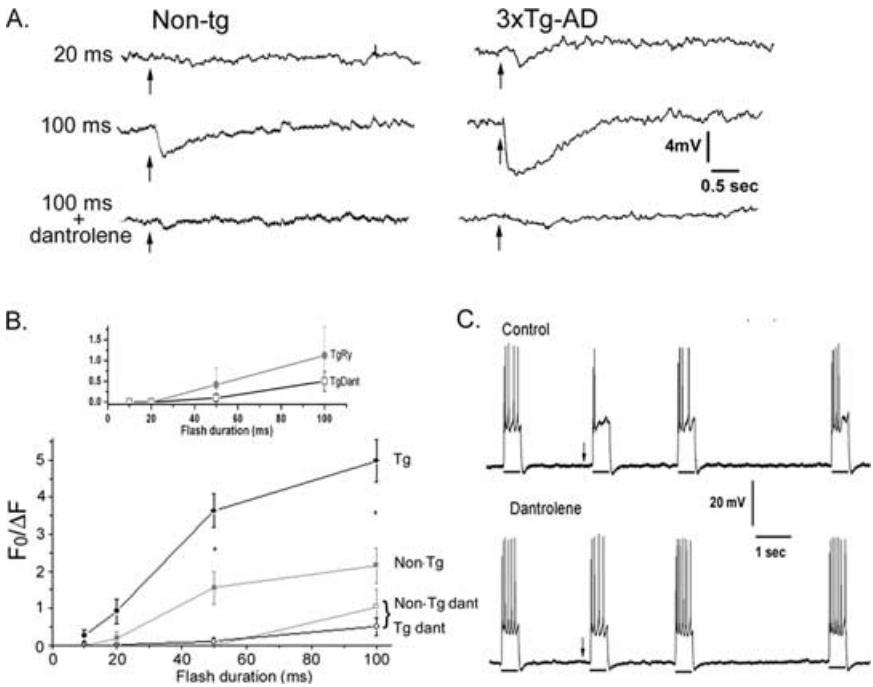

FIGURE 4. IP_3-evoked membrane hyperpolarizations are strongly suppressed by dantrolene. (**A**) Traces show (*from top to bottom*) changes in membrane potential in representative neurons from non-Tg (*left*) and 3×Tg-AD mice (*right*) following photolysis flashes of 20 and 100 ms duration, and the almost complete block of the response to a 100 ms flash in the presence of dantrolene (10 μM). (**B**) Relationships between photolysis flash duration and magnitude of the IP_3-evoked hyperpolarization. Main graph shows data from non-Tg (n =17, *black squares*) and Tg neurons (n = 31, *gray circles*), before (*filled symbols*) and during (*open symbols*) dantrolene application. Inset: Mean data comparing effects of ryanodine in Tg neurons (n = 16; *closed circles*) with dantrolene in Tg neurons (*open squares*, same data as in the main graph). (**C**) IP_3-mediated reduction in spiking frequency is suppressed by dantrolene. The upper trace shows spikes evoked by periodic injections of depolarizing current. A photolysis flash (100 ms) was delivered at the arrow to photorelease IP_3, resulting in a reduced spiking frequency for several seconds. The lower trace was obtained using the same protocol in the same neuron while continually superfusing dantrolene (10 μM).

were substantially abolished by dantrolene (FIG. 4 A, lower traces), even in the 3×Tg-AD neuron following a strong (100 ms) flash. Mean data for non-Tg and Tg neurons in control and dantrolene conditions are plotted in FIGURE 4 B. Hyperpolarizing responses in both non-Tg and Tg neurons increased with increasing photorelease of IP_3 but, for a given flash duration, the responses in Tg neurons were nearly three times as large (3.04-fold with 50 ms flashes, $P < 0.01$: and 2.7-fold with 100 ms flashes, $P \leq 0.01$). After adding dantrolene, only small IP_3-evoked hyperpolarizations remained with the strongest flashes, and were not significantly different between non-Tg and Tg neurons ($P > 0.05$).

IP_3-evoked changes in membrane conductance strongly regulate spiking patterns, and photorelease of IP_3 caused a long-lasting reduction in numbers of action potentials evoked by depolarizing current pulses (FIG. 4 C, upper trace). This modulation was abolished by dantrolene (FIG. 4 C, lower trace).

AD-Linked Mutations Affect the Coupling between RyR and Membrane K^+ Channels

The greater IP_3-evoked membrane hyperpolarization seen in neurons expressing AD-linked mutations might arise directly as a consequence of the enhanced ER Ca^{2+} release. However, this appears not to be the sole mechanism, because scatter graphs plotting the relationship between IP_3-evoked hyperpolarization amplitude ($-\Delta$mV) and the accompanying IP_3-evoked Ca^{2+} signals ($F_0/\Delta F$) revealed markedly different slopes between non-Tg and Tg neurons for both soma (FIG. 5 A) and dendrite (FIG. 5 B). That is to say, a given cytosolic Ca^{2+} signal was associated with a larger membrane hyperpolarization in Tg neurons, suggesting that the AD-linked mutations modulate the "coupling efficiency" between cytosolic Ca^{2+} signals and activation of membrane K^+ conductance, as well as enhancing the Ca^{2+} signals.

To explore the mechanism underlying this effect, we constructed a similar scatter plot of hyperpolarization *versus* Ca^{2+} signal amplitude after adding dantrolene to block RyR (FIG. 5 C). As noted before, both Ca^{2+} and membrane potential signals were strongly reduced, requiring pooled measurements from the soma and dendrite to obtain sufficient data points. Regression lines showed a slope for non-Tg neurons that was not appreciably different from that in control conditions without dantrolene, whereas in Tg neurons the slope was dramatically reduced as a result of blocking RyR. Our findings are further summarized in FIGURE 5 D. Key points are: (1) The slope of the relationship between membrane hyperpolarization ($-\Delta V$) and Ca^{2+} ($F_0/\Delta F$) was steeper (5.9) in Tg than in non-Tg neurons (3.15). (2) The slope in Tg neurons was greatly reduced by dantrolene, but was almost unchanged in non-Tg neurons. (3) The amplitudes of IP_3-evoked Ca^{2+} signals (measured from the soma, averaged across all flash durations) in Tg neurons were approximately double that in

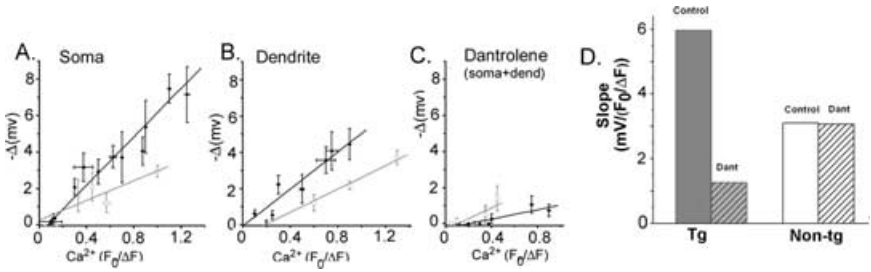

FIGURE 5. The relationship between the IP_3-evoked Ca^{2+} signal and membrane hyperpolarization is steeper in Tg than in non-Tg neurons. (**A**) Scatter plot showing the relationship between IP_3-evoked Ca^{2+} signal in the soma and the magnitude of the accompanying membrane hyperpolarization in neurons from non-Tg mice (n =14; *open symbols, gray line*) and Tg mice (n = 23; *closed symbols, black line*). Points show means ± 1 SEM obtained after binning over selected ranges of fluorescence amplitudes. (**B**) Corresponding data for measurements in the proximal dendrites. (**C**) Corresponding data in dantrolene (10 μM), obtained after pooling data from soma and dendrites. (**D**) Dantrolene strongly reduces the slope of the relationship between IP_3-evoked membrane hyperpolarization and Ca^{2+}-fluorescence signal in Tg neurons, but has negligible effect in non-Tg neurons. Slope data were derived from the plots in (**A**, **B**, **C**).

non-Tg neurons, whereas membrane hyperpolarizations were more than three times larger. (4) Thus, RyR are critically involved in mediating the hyperpolarizing response evoked by IP_3. Moreover, AD-linked mutations appear to result in greater hyperpolarizing responses not only because they enhance the Ca^{2+} signals, but also as a result of enhanced coupling efficiency between RyR and Ca^{2+}-activated K^+ conductance.

DISCUSSION

Involvement of RyR in IP_3-Mediated Signaling in Neuronal Physiology and Pathophysiology

The functional roles of intracellular Ca^{2+} stores in neuronal signaling are becoming increasingly recognized, and include modulation of membrane excitability,[18,20] synaptic activity and plasticity,[21] and gene transcription.[22] To gain a more complete understanding of these intracellular Ca^{2+} signaling mechanisms we attempted to parse their IP_3R and RyR components so as to identify interactions between the two types of release channel and determine functions that may specifically be coupled to a particular channel.

Here, we show that Ca^{2+} release evoked by IP_3 in cortical neurons from non-Tg mice arises primarily from Ca^{2+} flux through IP_3 receptors themselves, with a modest additional component being added by Ca^{2+} flux through RyR.

This balance, however, changes dramatically in transgenic mice expressing AD-linked mutations. *Presenilin* mutations are known to exaggerate ER-mediated Ca^{2+} signaling in a variety of cell types, but this has implicitly been assumed to arise as a direct consequence of increased flux specifically through IP_3R channels.[9–11] Instead, our results demonstrate that Ca^{2+} flux through RyR accounts for the great majority of the exaggerated IP_3-evoked Ca^{2+} response in AD transgenic mice. Consistent with this, neurons from AD transgenic mice showed larger Ca^{2+} signals in response to the RyR agonist caffeine, and enhanced expression of cortical RyR levels. Interestingly, in the AD transgenic mice, the RyR component associated with VGCC activation was not different from the non-Tg. Thus, the enhancement of Ca^{2+} signals by AD-linked mutations appears to arise primarily as a result of exaggerated Ca^{2+} flux through RyR rather than through IP_3R, and specifically affects ER Ca^{2+} signaling.

The RyR-mediated component of the intracellular Ca^{2+} signals almost certainly arises because CICR through RyR is triggered by, and amplifies, the Ca^{2+} liberated through IP_3R. Increased expression of RyR, as observed previously in cultured neurons[13,14] and in the brains of mice expressing the $PS1_{M146V}$ mutation,[19] provides a likely explanation for the exaggerated IP_3-evoked Ca^{2+} signals. Moreover, CICR may be further enhanced by the actions of *PS1* mutations to enhance Ca^{2+} filling of ER stores because elevated lumenal [Ca^{2+}] is known to increase the sensitivity of RyR to both cytosolic Ca^{2+} and caffeine.[23,24] Although increased store filling might also be expected to result in greater Ca^{2+} flux through IP_3R—as has been observed in *Xenopus* oocytes, which lack RyR[10]—our present results may be reconciled if Ca^{2+} stores in cortical neurons are enhanced sufficiently to sensitize RyR, while causing only a modest increase in Ca^{2+} flux through IP_3R. Questions remain, however, as to why the Ca^{2+} signals evoked by action potentials show relatively little RyR-mediated contribution; and why there is no appreciable enhancement of these signals in the transgenic mouse models of AD. An explanation may be that the voltage-gated Ca^{2+} channels in the plasma membrane are located more distantly from RyR than are the IP_3R-channels, and are thus relatively ineffective in inducing CICR.

The mechanisms by which mutations in *PS* expression result in RyR upregulation and exaggerated ER Ca^{2+} release are presently unclear. One explanation draws on evidence showing that the *PS* mutations result in altered γ-secretase activity, which is responsible for the proteolysis of amyloid precursor protein (APP).[7] APP proteolysis generates several fragments, including the APP-intracellular domain fragment (AICD), which has been shown to regulate IP_3-mediated Ca^{2+} signaling by possible transcriptional mechanisms.[25,26] Although the target proteins ultimately affected are not known in this case, the AICD transcriptional activity may serve to influence expression or function of the RyR.

Electrical Excitability Is Modulated by RyR

Intracellular Ca^{2+} plays an important role in modulating the electrical excitability of neurons, and AD-linked disruptions in Ca^{2+} might thus be expected to have acute consequences for neuronal signaling, as well as for chronic disease pathology. Accordingly, we had found that hyperpolarizing responses to IP_3 are enhanced in $PS1_{KI}$ neurons,[11,19] probably because the enhanced cytosolic Ca^{2+} signals evoke greater activation of Ca^{2+}-dependent membrane K^+ channels. We now show a similar exaggeration of IP_3-evoked hyperpolarizing responses in 3×Tg-AD neurons, and further demonstrate that in 3×Tg-AD, PS_{KI}, and non-Tg mice these membrane responses are mediated primarily by Ca^{2+} liberated through RyR, rather than by the Ca^{2+} directly liberated through IP_3R. In particular, blocking of RyR greatly reduced IP_3-evoked hyperpolarizations in both non-Tg and Tg neurons, resulting in almost identical membrane responses to a given flash duration.

The larger hyperpolarizing responses in the Tg neurons could most simply be accounted for as a direct consequence of the greater overall Ca^{2+} signal. However, this appears not to be the sole explanation, because the membrane responses accompanying Ca^{2+} signals of a given size were roughly twice as large in Tg versus non-Tg neurons: in other words, the Tg neurons showed a greater "coupling efficiency" between cytosolic Ca^{2+} and activation of Ca^{2+}-dependent K^+ current. This may result if sites of Ca^{2+} liberation through RyR are closer to the Ca^{2+}-dependent K^+ channels than are the sites of IP_3R-mediated Ca^{2+} liberation. On this basis, the disproportionate hyperpolarization in Tg neurons arises because most of their exaggerated Ca^{2+} signal arises through RyR; whereas after blocking RyR both Tg and non-Tg neurons show comparably small hyperpolarizations that are driven by the remaining IP_3R-mediated Ca^{2+} liberation.

CONCLUSIONS

Our results reveal important new aspects of Ca^{2+} signaling disruptions associated with AD. Specifically, exaggeration of IP_3-evoked neuronal Ca^{2+} signals is principally linked to mutations in *presenilin* and is largely independent of expression of Aβ plaques or neurofibrillar tangles; these exaggerated signals are manifest throughout life and do not represent an acceleration of a normal aging process; and they arise principally through enhanced Ca^{2+} flux through RyR, not IP_3R. Several crucial questions remain unanswered, including the mechanism by which mutations in *presenilin* modulate RyR-mediated signaling, and whether and how dysregulated Ca^{2+} signaling may play a causative role in AD pathology. Nonetheless, these findings further strengthen the growing

consensus that a calciumopathy may be at least partly responsible for neuronal degeneration in AD.

REFERENCES

1. BERRIDGE, M., M. BOOTMAN & P. LIPP. 1998. Calcium—a life and death signal. Nature **395:** 645–649.
2. BERRIDGE, M., P. LIPP & M. BOOTMAN. 2000. The versatility and universality of calcium signaling. Mol. Cell Biol. **1:** 11–21.
3. FINCH, E., T. TURNER & S. GOLDIN. 1991. Calcium as a coagonist of inositol 1,4,5-triphosphate-induced calcium release. Science **252:** 443–446.
4. YAO, Y. & I. PARKER. 1992. Potentiation of inositol trisphosphate-induced Ca^{2+} mobilization in Xenopus oocytes by cytosolic Ca^{2+}. J. Physiol. **458:** 319–338.
5. FRIEL, D.D. & R.W. TSIEN. 1992. A caffeine- and ryanodine-sensitive Ca^{2+} store in bullfrog sympathetic neurones modulates effects of Ca^{2+} entry on $[Ca^{2+}]_i$. J. Physiol. **450:** 217–246.
6. MATTSON, M. *et al*. 2000. Calcium signaling in the ER: its role in neuronal plasticity and neurodegenerative disorders. TINS **23:** 222–229.
7. LAFERLA, F.M. 2002. Calcium dyshomeostasis and intracellular signaling in Alzheimer's disease. Nat. Rev. Neurosci. **3:** 862–872.
8. STUTZMANN, G.E. 2005. Calcium dysregulation, IP_3, signaling and Alzheimer's disease. Neuroscientist **11:** 110–115.
9. GUO, Q. *et al*. 1996. Alzheimer's PS-1 mutation perturbs calcium homeostasis and sensitizes PC12 cells to death induced by amyloid beta-peptide. Neuroreport **8:** 379–383.
10. LEISSRING, M.A. *et al*. 1999. Alzheimer's presenilin-1 mutation potentiates inositol 1,4,5-trisphosphate-mediated calcium signaling in Xenopus oocytes. J. Neurochem. **72:** 1061–1068.
11. STUTZMANN, G.E. *et al*. 2004. Dysregulated IP_3 signaling in cortical neurons of knock-in mice expressing an Alzheimer's-linked mutation in presenilin1 results in exaggerated Ca^{2+} signals and altered membrane excitability. J. Neurosci. **24:** 508–513.
12. ETCHEBERRIGARAY, R. *et al*. 1998. Calcium responses in fibroblasts from asymptomatic members of Alzheimer's disease families. Neurobiol. Dis. **5:** 37–45.
13. CHAN, S. *et al*. 2000. Presenilin-1 mutations increase levels of ryanodine receptors and calcium release in PC12 cells and cortical neurons. J. Biol. Chem. **275:** 18195–18200.
14. SMITH, I. *et al*. 2005. Enhanced caffeine-induced Ca^{2+} release in the 3xTg-AD mouse model of Alzheimer's disease. J. Neurochem. **94:** 1711–1718.
15. POPESCU, B. *et al*. 2004. Gamma-secretase activity of presenilin 1 regulates acetylcholine muscarinic receptor-mediated signal transduction. J. Biol. Chem. **279:** 6455–6464.
16. ODDO, S. *et al*. 2003. Triple-transgenic model of Alzheimer's disease with plaques and tangles: intracellular Abeta and synaptic dysfunction. Neuron **39:** 409–421.
17. SAH, P. 1996. Ca^{2+}-activated K^+ currents in neurones: types, physiological roles and modulation. TINS **19:** 150–154.

18. STUTZMANN, G., F. LAFERLA & I. PARKER. 2003. Ca^{2+} signaling in mouse cortical neurons studied by two-photon imaging and photoreleased inositol triphosphate. J. Neurosci. **23:** 758–765.
19. STUTZMANN, G.E. *et al*. 2006. Enhanced ryanodine receptor recruitment contributes to Ca2+ disruptions in young, adult, and aged Alzheimer's disease mice. J. Neurosci. **26:** 5180–5189.
20. DAVIES, P., D. IRELAND & E. MCLACHLAN. 1996. Sources of Ca^{2+} for different Ca^{2+}-activated K^{+} conductances in neurones of the rat superior cervical ganglion. J. Physiol. **495:** 353–366.
21. NAKAMURA, T. *et al*. 2000. Inositol 1,4,5-triphosphate (IP_3)-mediated Ca^{2+} release evoked by metabotropic agonists and backpropagating action potentials in hippocampal CA1 pyramidal neurons. J. Neurosci. **20:** 8365–8376.
22. MELLSTROM, B. & J. NARANJO. 2001. Mechanisms for Ca^{2+} -dependent transcription. Curr. Opin. Neurobiol. **11:** 312–319.
23. SHMIGOL, A. *et al*. 1996. Gradual caffeine-induced Ca^{2+} release in mouse dorsal root ganglion neurons is controlled by cytoplasmic and luminal Ca^{2+}. Neuroscience **73:** 1061–1067.
24. KOIZUMI, S. *et al*. 1999. Regulation of ryanodine receptor opening by lumenal Ca^{2+} underlies quantal Ca^{2+} release in PC12 cells. J. Biol. Chem. **274:** 33327–33333.
25. CAO, X., T.C. SUDHOF. 2001. A transcriptively active complex of APP with Fe65 and histone acetyltransferase Tip60. Science **293:** 115–120.
26. LEISSRING, M. *et al*. 2002. A physiologic signaling role for the gamma-secretase-derived intracellular fragment of APP. Proc. Natl. Acad. Sci. **99:** 4697–4702.